SYSTEMATIC SOLAR PVT TESTING IN STEADY-STATE AND DYNAMIC OUTDOOR CONDITIONS

Guarracino I.[a], Freeman J.[a], Ramos A.[a], Kalogirou S.A.[b], Ekins-Daukes N.[c] and Markides C.N.[a]*
[a]Clean Energy Processes (CEP) Laboratory, Department of Chemical Engineering, Imperial College London, London, UK
[b]Department of Mechanical Engineering and Materials Science and Engineering, Cyprus University of Technology, Limassol, Cyprus
[c]Blackett Laboratory, Department of Physics, Imperial College London, London, UK
*E-mail: c.markides@imperial.ac.uk

ABSTRACT

In order to predict accurately the performance of solar-thermal or hybrid PVT systems, it is necessary that the steady-state and dynamic performance of the collectors is understood. This work focuses on the testing and detailed characterization of non-concentrating PVT collectors based on the testing procedure specified in the European standard EN 12975-2. Three different types of PVT collectors were tested in Cyprus under outdoor conditions similar to those specified in the standard. Amongst other results, we show that that poor thermal contact between the laminate and the copper absorber can lead to a significant deterioration in thermal performance and that a glass cover improves the thermal performance by reducing losses as expected, but causes electrical losses that vary with the glass transmittance and the incident angle. It is found that the reduction in electrical efficiency at large solar incidence angles is more significant than that due to elevated temperatures representative of water heating applications. Dynamic tests are performed by imposing a step change in incident irradiance in order to quantify the collector time constant and effective heat capacity. A time constant of ~ 8 min is found for a commercial PVT module, which compares to < 2 min for a flat plate solar collector. The PVT collector time constant is found to be very sensitive to the thermal contact between the PV layer and the absorber, which may vary according to the quality of construction, and also to the operating flow rate.

INTRODUCTION

Non-concentrating solar photovoltaic (PV) systems are a mature technology that is highly suitable for the generation of electricity, while non-concentrating and low-concentration solar-thermal systems can provide thermal energy for water, space heating, and low-temperature process heating or cooling [1, 2]. Hybrid thermal-PV (PVT) collectors combine PV modules with a heat recovery configuration and provide simultaneous electrical and thermal outputs from the same collector area [3–5]. In order to predict correctly the performance of solar-thermal systems, collectors must be characterized in terms of their steady-state and dynamic performance [6]. Suitable testing methods for conventional solar-thermal collectors, such as those in the European Standard EN 12975-2 [7], are well established and test data is widely available. By comparison, the PVT market is relatively small at present and test data for these collectors is scarce.

Recently, several authors have focused on the experimental characterization of PVT collectors aiming to obtain reliable data on their operation and performance. Most of the data are available for low-temperature unglazed collectors and focus on the potential improvement of the thermal contact [8, 9] and on reducing the heat loss coefficient with a glass cover [10]. Lammle *et al.* [11] recently investigated the effect of the solar cell emissivity on the thermal efficiency of a glazed PVT collector by applying a selective coating on the solar cells that reduces the heat losses by 80% while the electrical output drops by only 3%. In another attempt to improve thermal efficiency, the use of nano-ferrofluids is proposed in Ref. [12], and silica/water nanofluids have been proposed in Ref. [13].

The aim of the present paper is to establish a procedure for the testing of PVT collectors under real weather conditions in

NOMENCLATURE

A	[m^2]	Area
a_1, a_2	[W/m^2 K, W/m^2 K^2]	Collector heat loss coefficients
C	[J/K]	Effective heat capacity
c	[J/kg K]	Specific heat capacity
I_{sc}	[A]	Short circuit current
M	[kg]	Mass
$\dot{m}$	[kg/s]	Mass flow rate
T	[°C]	Temperature
t	[s]	Time
T_m^*	[m^2 K/W]	Reduced temperature
P(MPP)	[W]	Maximum PV power
T_0	[°C]	PV reference temperature
T_a	[°C]	Ambient temperature
$\overline{T}_c$	[°C]	Mean collector temperature
$T_{f\text{-}i}$, $T_{f\text{-}o}$	[°C]	Fluid inlet and outlet temperatures
T_{PV}	[°C]	PV temperature
V_{oc}	[V]	Open circuit voltage
Greek symbols		
β	[K^{-1}]	PV temperature coefficient
η_E	[-]	Electrical efficiency
η_{TH}	[-]	Thermal efficiency
η_0	[-]	Optical efficiency
τ	[-]	Transmittance, time constant
θ	[rad]	Incidence angle

steady-state and dynamic operation, and to identify the main design and operating parameters influencing their performance. Glazed and unglazed PVT collectors are tested and the effect of the glass cover and the thermal contact between the PV module and the rear absorber is analysed. The dynamic behaviour of the PVT collectors is also investigated using the experimental and calculation-based methods from the European Standard. The accurate prediction of solar collector behaviour is of fundamental importance for ensuring that the system is designed properly and does not under-perform or fail; while improved models of PVT systems are required for optimization of the design and operating parameters in order to achieve higher electrical and thermal energy yields and increased energy savings. The previous studies cited above focused on the steady-state performance of PVT collectors, whereas it is demonstrated here that hybrid collectors are characterized by a large thermal mass and thus the effective heat capacity should be quantified for accurate prediction of performance under time-varying irradiance conditions.

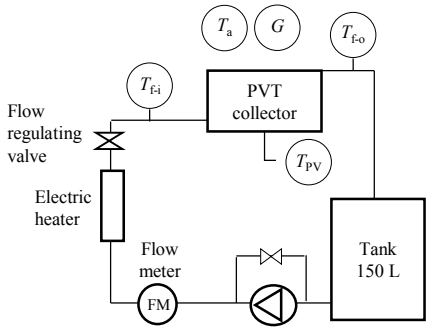

Figure 1: Schematic of the closed loop system.

Table 1: Specifications of the commercial PVT module M1, and of the solar thermal collector, PV thin film module and glass layer used for collectors M2U, M2G and M3 [14–16].

Parameter	Unit	M1	M2U/M2G/M3
η_0	-	0.49	0.62
a_1	W m^{-2} K^{-1}	4.03	4.24
a_1	W m^{-2} K^{-2}	0.07	0.01
C	kJ K^{-1}	20.0	14.6
η_{EL}	-	0.49	0.62
β	% K^{-1}	N/A	-0.4
V_{oc}	V	43.4	93.3
I_{sc}	A	5.5	1.7
P_e (MPP)	W	180	110
τ_g ($\theta = 0$)	-	N/A	0.95

EXPERIMENTAL METHODS

A series of tests were performed to characterize the thermal and electrical performance of four PVT collectors, each of a different design and construction. The collectors are shown in Figure 2, and include: a commercial PVT module (M1); an unglazed PVT module with 65% PV covering factor (M2U); a glazed PVT module with 65% PV covering factor (M2G); and a glazed module with 100% PV covering factor (M3). The tests were performed at the Cyprus University of Technology in Limassol, on a south oriented frame with 37° inclination angle. M2U, M2G and M3 were constructed in-house by installing a thin film module onto a solar thermal collector with or without the cover glass. The specifications the collectors are reported in Table 1. The tests were performed on the closed loop system shown in Figure 1 at around solar noon. During the tests the collector inlet and outlet temperatures, ambient temperature and irradiance on the collector plane were monitored at 1 s sampling rate. The following is a description of the methodology used for the steady-state and dynamic characterization of the solar collectors.

Steady-state collector characterization

The steady-state efficiency is obtained by testing the collector over a range of inlet temperatures at incidence angle $\leq 20°$ and global irradiance greater than 800 W/m^2, as specified in EN 12975-2 [7]. In order to compare the thermal efficiency of the different collectors, the flow rate per unit area was kept at 0.02 kg/s m^2 during all tests while the PVT electrical output is maintained at the maximum power point. The steady-state collector efficiency is obtained as follows:

$$\eta_{TH} = \frac{\dot{m}c(T_{f\text{-}o} - T_{f\text{-}i})}{GA} = \eta_o - a_1 T_m^* - a_2 G T_m^{*2}. \quad (1)$$

In order to determine the coefficients η_o, a_1, a_2 according to EN12975-2 [7] the instantaneous thermal efficiency is plotted against the reduced mean temperature $T_m^* = \frac{(\overline{T}_c - T_a)}{G}$, where $\overline{T}_c$ is the average of the measured inlet and outlet temperatures, and a second-order least-squares fit is applied to the data.

The electrical efficiency is evaluated by measuring the electrical power at the maximum power point with a PVPM 2540C *I-V* curve-tracing device. In PVT modules, the electrical efficiency decreases with the module temperature according to [17, 18]:

$$\eta_E = \eta_0[1 - \beta(T_{PV} - T_0)], \quad (2)$$

where T_{PV} is the PV temperature, β the temperature coefficient (0.004 K^{-1} for c-Si cells) , and η_0 is the electrical efficiency at a reference temperature T_0 [17, 18].

Dynamic collector characterization

The time-varying behaviour of the collector is described by Equation 3, which is a modifications of the steady-state efficiency equation to include a time-derivative term and the effective heat capacity parameter C:

$$\dot{m}c(T_{f\text{-}o} - T_{f\text{-}i}) = \eta_o AG - a_1 A(\overline{T}_c - T_a) - a_1 A(\overline{T}_c - T_a)^2 - C\frac{d\overline{T}_c}{dt}$$
$$\approx \eta_o AG - UA(\overline{T}_c - T_a) - C\frac{d\overline{T}_c}{dt}. \quad (3)$$

A method for estimating C is presented in EN 12975-2, in which the thermal capacity of each component of the collector is multiplied by a weighting factor p that describes the degree of thermal interaction it has with the circulating fluid. The total

Figure 2: PVT collectors: M1 (left), and M2U (right).

effective thermal capacity of the collector is found by summing the weighted thermal capacities of each n component:

$$C_{\mathrm{wt}} = \sum p_n m_n c_n \,. \tag{4}$$

An experimental method for evaluating C is also presented in EN 12975-2. In this method, the collector is exposed to a step-change in irradiance and the time taken for the collector outlet temperature to reach a new steady-state value is measured (while the inlet temperature is maintained at a constant value). Then, by integrating and rearranging Equation 3:

$$C_{\mathrm{exp}} = \frac{A\eta_{\mathrm{o}} \int_{t1}^{t2} G\mathrm{d}t - \dot{m}c \int_{t1}^{t2} \Delta T_{\mathrm{f}}\mathrm{d}t - AU\left[\int_{t1}^{t2} (T_{\mathrm{f-i}} - T_{\mathrm{a}})\mathrm{d}t + 0.5\int_{t1}^{t2} \Delta T_{\mathrm{f}}\mathrm{d}t\right]}{\overline{T}_{\mathrm{c},2} - \overline{T}_{\mathrm{c},1}} \,. \tag{5}$$

The time constant τ_{s} is also evaluated from the dynamic response of the collector to a step variation of the input, this is the elapsed time that is required to reach a ΔT of 63.2% of the final steady state from the initial steady-state conditions.

RESULTS

Steady-state thermal and electrical efficiency

The steady-state tests were performed under irradiance variations between 650 W/m^2 and 910 W/m^2 in July, and inlet-temperature variations between 32 °C and 76 °C. The thermal efficiency of M2U and M2G is shown in Figure 3. From these results it is evident that adding a glass layer results in an improvement in the thermal efficiency. The heat loss coefficient U of the glazed PVT module M2G is 2.17 W/m^2 K, while for the unglazed PVT M2U it is 8.37 W/m^2 K.

The electrical efficiency of M2U decreases linearly with the mean fluid temperature as shown in Figure 4a. A temperature coefficient of 0.14 %/K was obtained from a linear fit of this efficiency against collector temperature, which is lower than the

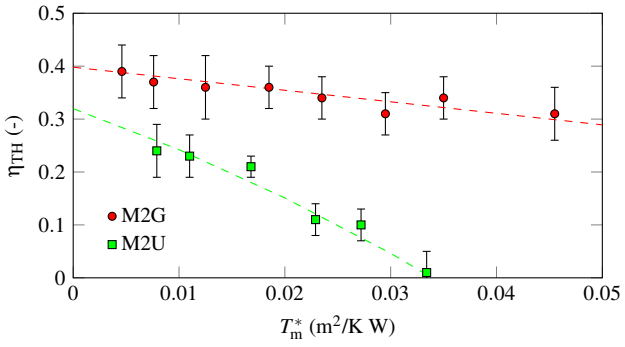

Figure 3: Thermal efficiency of M2U and M2G panels.

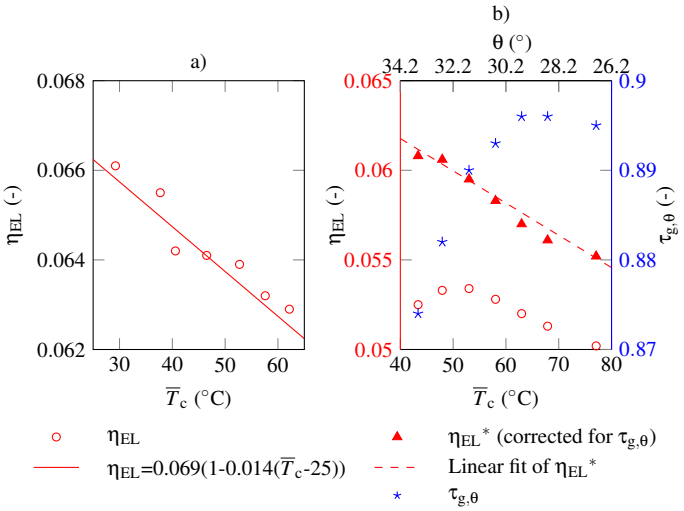

Figure 4: Electrical efficiency η_{EL} of a) M2U, plotted as a function of the mean fluid temperature; and b) M2G, plotted as a function of the fluid temperature and glass transmittance (dependent on solar incidence angle).

value stated in the PV module specification sheet of 0.35 %/K; although it should be noted that the former is based on the average fluid temperature measured between the inlet and outlet, while the latter on the PV cell temperature.

The electrical efficiency of M2G is on average 20% lower than the electrical efficiency of the unglazed version. The reflection from the unglazed PV module is 10%, while the total reflection from the glazed PVT module is 12% at normal incidence corresponding to a glass transmittance of 0.95 [19]. However, the glass-layer transmittance is significantly reduced at larger incidence angles, leading to further losses in electrical performance. Moreover, this is found to have a notable affect on the results, as shown in Figure 4b. During the hours over which the tests were performed (between 10:47 a.m. and 1:20 p.m.), the smallest incidence angle (27°) corresponds to a transmittance value of 0.91, while the largest incidence angle (∼35°) corresponds to a lower

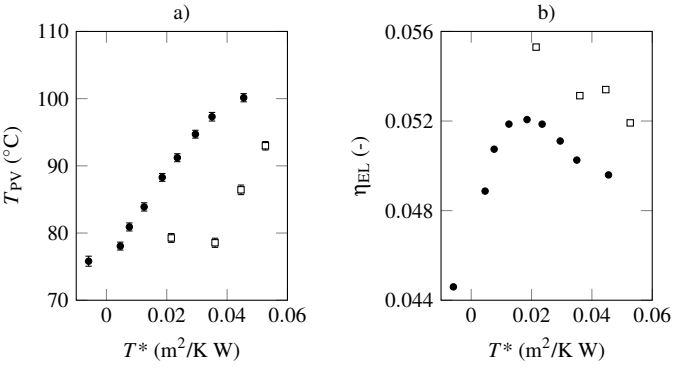

Figure 5: a) PV temperature, and b) electrical efficiency of glazed collector M2G. Black circles show default configuration, white squares show modified configuration with thermal grease to improve thermal contact between PV layer and absorber.

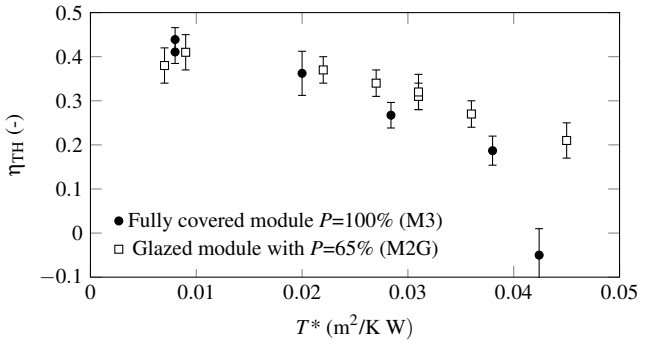

Figure 6: Comparison of the thermal efficiency of the PVT module with 100% and 65% covering factor.

transmittance value of 0.81. At the lowest collector temperature, for which the electrical efficiency would ordinarily be highest, the larger incidence angle corresponds to a reduced glass transmittance (shown by the star points) and the result is a decrease in electrical efficiency (shown by the circular points). So the point where the maximum electrical efficiency occurs is a combination of the cells temperature and incidence angle.

The electrical efficiency can be corrected for the angular glass transmittance using Equation 6:

$$\eta_{EL}{}^{*} = \frac{\eta_{EL}}{\tau_g(\theta)}, \tag{6}$$

resulting in the values indicated by the solid triangle points in Figure 4b. The corrected results show the expected linear trend of decreasing electrical efficiency with increasing temperature and good agreement with the results from the unglazed collectors.

Sensitivity to thermal contact and covering factor

For the M2G collector, improvements were made to the thermal contact between the PV layer and the thermal absorber by applying a silicon paste with a thermal conductivity of 2.3 W/m K, and the effect on the thermal and electrical performance was investigated. It was found that an improvement in thermal efficiency could not be observed conclusively beyond the margin of experimental error; however Figure 5a shows that the application of the paste results in a $\sim$10 °C lower temperature measured on the PV layer. This in turn results in a 6 – 8% relative improvement in electrical efficiency, as shown in Figure 5b.

Only 65% of the M2G thermal-absorber area was covered by PV cells, leaving the remaining area at the top of the collector exposed (see Figure 2). The effect on the thermal performance of increasing the PV covering factor to 100% was investigated for the M3 collector by using a reflective thermal insulator to cover the exposed absorber area. The thermal efficiency of M3 was found to be similar to M2G at low values of T_m^* but shows a more substantial deterioration at increased fluid temperatures, (see Figure 6). It should be noted that the emissivity of the PV layer is high compared with the selective-coated copper absorber ($\sim$0.8 compared to $\sim$0.2 [18]), resulting in increased radiative losses at higher operating temperatures from the PV layer.

Table 2: Solar collector effective heat capacity and time constant values, obtained according to the experimental and calculation-based methods in EN 12975-2 [7].

Collector	C_{wt} (kJ/K)	C_{exp} (kJ/K)	τ_{exp} (s)
FPC	11.6	21.6	107
PVT, M1	24.3	129.6	474
PVT, M2U	23.6	31.5	103
PVT, M2G	23.8	90.7	90

Dynamic testing results

The PVT modules were tested in dynamic conditions in order to obtain an experimental value of the effective heat capacity C_{exp} and the collector time constant τ_{exp}. As an example, the temperature evolution for the M1 collector is plotted in Figure 7. Comparison values of the effective heat capacity C_{wt} were also calculated using the weighting-factor method. The results are reported and compared in Table 2. As can be seen from Table 2 the time constant for the PVT, M1 collector is 474 s (about 8 min).

For all collectors, a large discrepancy is found between the values of C obtained from the experimental and calculation-based methods, with the former being 2 – 5 times larger than those obtained from the more common weighted-component calculation method. Dynamic tests revealed a slower thermal-response for the PVT collectors (with the slowest time constant of $\sim$8 min) compared to a conventional thermal-only flat-plate collector ($<$ 2 min). These tests also revealed a 46% increase in the effective thermal capacity for the M2U collector compared to the FPC as a result of the addition of the PV layer. This relative increase was relatively well predicted by the weighted-component calculation method. However, a more significant (188%) increase in C_{exp} was observed between the M2U and M2G as a result of the addition of the glazed layer. The extent of this increase was under-predicted by the weighted-component calculation method, due to the very low weighting factor (0.014) recommended for the glazing in EN 12975-2 [7]. For a PVT collector, the degree of thermal interaction with the glazed layer may be more significant due to the higher emissivity of the PV layer compared to the selectively-coated metal absorber, resulting in a higher proportion of the absorbed thermal energy re-radiated to the glass layer. Furthermore, the mass of the PVT collectors is higher than that of the solar thermal collector due to the addition of the PV module (for M1, M2U and M2G the mass is 37%, 3% and 64% higher than the mass of FPC).

The commercial PVT collector M1 was found to have the largest heat capacity and time constant due to certain design and construction features, including small tube diameters act to that limit operation to low flow-rates. Inspection of the collector also revealed a poor thermal contact between the PV and thermal absorber resulting in poor heat transfer to the fluid.

From a practical perspective, repeatability of results from the experimental method was difficult to achieve in an outdoor setting and the results were sensitive to environmental conditions making outdoor testing particularly challenging and time-consuming. The time taken for the PVT collectors to reach

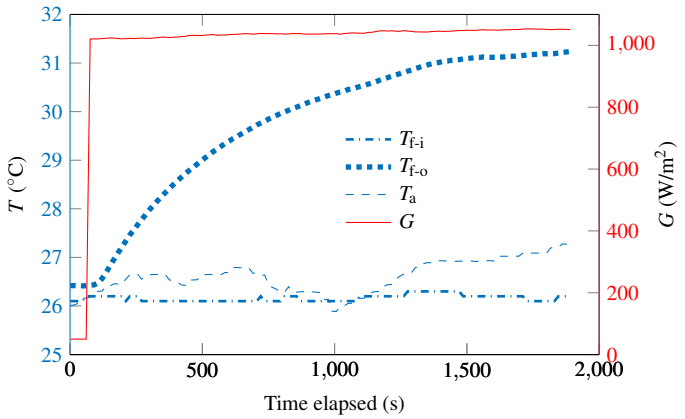

Figure 7: Temperatures and irradiance monitored during a dynamic test on M1.

steady state when exposed to a step-change in irradiance was as long as 30 min, suggesting that dynamic characterisation of PVT collectors using such a method could prove expensive compared to flat-plate thermal collectors with lower thermal inertias. Thus an accurate predictive model might be preferred for the evaluation of both the steady-state and the dynamic behaviour of PVT collectors to avoid lengthy and expensive testing.

CONCLUSIONS

The effect of various design features on electrical and thermal efficiency was investigated experimentally on a range of PVT collectors. The addition of a glass cover resulted in a considerable improvement in thermal performance, with the heat loss coefficient decreasing from 8.4 to 2.2 W m^{-2} K^{-1}. On the other hand, the increased reflection losses led a to a 10 – 20% reduction in electrical output that is most notable at larger incidence angles. Enhancements to the thermal contact between the PV layer and the rear absorber increases the thermal efficiency of the PVT collector and was found to result in a $\sim$10 °C lower operating temperature measured at the PV layer.

Dynamic tests on PVT collectors revealed large a discrepancy between directly measured effective heat capacities and those obtained from calculation-based methods, with PVT collectors characterized by much slower responses to time varying inputs in comparison to solar thermal collectors of the same area.

ACKNOWLEDGEMENT

This work was supported by the UK Engineering and Physical Sciences Research Council (EPSRC) [grant number EP/M025012/1]. The authors would also like to acknowledge the EU Climate-KIC http://www.climate-kic.org for IG's PhD studentship. Data supporting this publication can be obtained on request from cep-lab@imperial.ac.uk.

REFERENCES

[1] Markides, C. N., Low-concentration solar-power systems based on organic Rankine cycles for distributed-scale applications: Overview and further developments, *Frontiers in Energy Research*, 2015, pp. 47

[2] Freeman, J., Hellgardt, K., and Markides, C.N., An assessment of solar-powered organic Rankine cycle systems for combined heating and power in UK domestic applications, *Applied Energy*, Vol. 138, 2015, pp. 605-620

[3] Kalogirou, S. A. and Tripanagnostopoulos, Y., Hybrid PV/T solar systems for domestic hot water and electricity production, *Applied Energy*, Vol. 47, 2006, pp. 3368-3382

[4] Herrando, M., Markides, C. N. and Hellgardt, K., A UK-based assessment of hybrid PV and solar-thermal systems for domestic heating and power: System performance, *Applied Energy*, Vol. 122, 2014, pp. 288-309

[5] Herrando, M. and Markides, C. N., Hybrid PV and solar-thermal systems for domestic heat and power provision in the UK: Techno-economic considerations, *Applied Energy*, Vol. 161, 2016, pp. 512-532

[6] Guarracino, I., Mellor, A., Ekins-Daukes, N. J. and Markides, C. N., Dynamic coupled thermal-and-electrical modelling of sheet-and-tube hybrid photovoltaic/thermal (PVT) collectors, *Applied Thermal Engineering*, Vol. 101, 2016, pp. 778-795

[7] European Standard EN 12975-2, European Committee for Standardisation, 2006

[8] Cremers, J., Mitina, I., Palla, N., Klotz, F., Jobard, X. and Eicker, U., Experimental Analyses of Different PVT Collector Designs for Heating and Cooling Applications in Buildings, *Energy Procedia*, Vol. 78, 2015, pp. 1889-1894.

[9] Jin-Hee, K. and Jun-Tae, K., The Experimental Performance of an Unglazed PVT Collector with Two Different Absorber Types, *International Journal of Photoenergy*, 2012.

[10] Kim, J. H. and Kim, J. T., Comparison of electrical and thermal performances of glazed and unglazed PVT collectors, *International Journal of Photoenergy*, Vol. 2012, 2012.

[11] Lämmle, M. , Kroyer, T., Fortuin, S., Wiese, M. and Hermann, M., Development and modelling of highly-efficient PVT collectors with low-emissivity coatings , *Solar Energy*, Vol. 130, 2016, pp. 161-173

[12] Ghadiri, M., Sardarabadi, M., Pasandideh-Fard, M. and Moghadam, A.J., Experimental investigation of a PVT system performance using nano ferrofluids, *Energy Conversion and Management*, Vol. 103, 2015, pp. 468-476

[13] Sardarabadi, M., Pasandideh-Fard, M. and Heris, S.Z., Experimental investigation of the effects of silica/water nanofluid on PV/T (photovoltaic thermal units, *Energy*, Vol. 66, 2014, pp. 264-272

[14] Eurofins – Modulo Uno S.P.A. Solar collector test report according to EN 12975-2: 2006. Online: http://intergeo.sk/

[15] Solar thermal collector technical specification, Elcora, 2010

[16] Technical specifications of Solibro SL2 module-Generation 1.5, 2017. Online: http://solibro-solar.com/

[17] Chow, T.T., Performance analysis of photovoltaic-thermal collector by explicit dynamic model, *Solar Energy*, Vol. 75, 2003, pp. 143-152

[18] Santbergen, R. and Van Zolingen, R.J.C., The absorption factor of crystalline silicon PV cells: A numerical and experimental study, *Solar Energy Materials and Solar Cells*, Vol. 92, 2008, pp. 432-444

[19] Duffie, J.A. and William, A.B., Solar engineering of thermal processes, 1974